Complex Cellular Responses of *Helicobacter pylori*-Colonized Gastric Adenocarcinoma Cells[∇]

Sabine Schneider,[1] Gert Carra,[1,3] Ugur Sahin,[2] Benjamin Hoy,[1,3]
Gabriele Rieder,[3] and Silja Wessler[1,3]*

*Junior Research Group, Paul-Ehrlich Institute, Langen, Germany[1]; Department of Internal Medicine III,
Experimental and Translational Oncology, Johannes Gutenberg University, Mainz, Germany[2]; and
Division of Microbiology, Paris-Lodron University, Salzburg, Austria[3]*

Helicobacter pylori is an important class I carcinogen that persistently infects the human gastric mucosa to induce gastritis, gastric ulceration, and gastric cancer. *H. pylori* pathogenesis strongly depends on pathogenic factors, such as VacA (vacuolating cytotoxin A) or a specialized type IV secretion system (T4SS), which injects the oncoprotein CagA (cytotoxin-associated gene A product) into the host cell. Since access to primary gastric epithelial cells is limited, many studies on the complex cellular and molecular mechanisms of *H. pylori* were performed in immortalized epithelial cells originating from individual human adenocarcinomas. The aim of our study was a comparative analysis of 14 different human gastric epithelial cell lines after colonization with *H. pylori*. We found remarkable differences in host cell morphology, extent of CagA tyrosine phosphorylation, adhesion to host cells, vacuolization, and interleukin-8 (IL-8) secretion. These data might help in the selection of suitable cell lines to study host cell responses to *H. pylori in vitro*, and they imply that different host cell factors are involved in the determination of *H. pylori* pathogenesis. A better understanding of *H. pylori*-directed cellular responses can provide novel and more balanced insights into the molecular mechanisms of *H. pylori*-dependent pathogenesis *in vivo* and may lead to new therapeutic approaches.

Helicobacter pylori has been identified as the causative agent associated with inducing inflammatory disorders, including chronic gastritis and peptic ulcer disease (4, 22). Chronic inflammation in response to *H. pylori* infection is characterized by mucosal infiltration of neutrophils and lymphocytes and represents the initial phase in carcinogenesis leading to gastric adenocarcinoma and mucosa-associated lymphoid tissue (MALT) lymphoma (7). However, knowledge of the detailed mechanisms resulting in *H. pylori*-associated disorders is still poor.

The risk of developing severe diseases is determined by the expression of *H. pylori* virulence factors. Among those factors, VacA, identified as an important pathogenic protein, is constitutively secreted and binds to receptor protein tyrosine phosphatase α (RPTPα) and RPTPβ on the epithelial cell surface. *In vivo*, these receptors are required for VacA-induced gastric ulceration (11). After binding, VacA is internalized and forms pores in the membrane as well as large vacuoles in the host cytoplasm (24).

H. pylori strains expressing genes carried on the cytotoxin-associated gene (*cag*) pathogenicity island (PAI) also have an enhanced pathogenic potential. Individuals infected with *cag* PAI-positive *H. pylori* strains display a more pronounced immune response involving a wide range of proinflammatory cytokines and chemokines, such as interleukin-1 (IL-1), IL-6, IL-8, and tumor necrosis factor alpha (TNF-α) (5, 9). Functionally, the *cag* PAI encodes a specialized secretion system

(type IV secretion system [T4SS]) which binds to β1-integrins on epithelial host cells, enabling *H. pylori* to translocate particular factors that are involved in inducing intracellular signaling cascades of host cells (15, 16). In this context, injected CagA becomes tyrosine phosphorylated by kinases of the Src and Abl families (23, 28) and induces drastic cellular elongation accompanied by migration of *H. pylori*-infected epithelial cells (26). The molecular mechanism by which CagA triggers the observed changes in cell morphology is still not fully understood, but translocated CagA obviously interferes with the functions of eukaryotic signaling proteins, leading to deregulation of focal adhesions and the actin cytoskeleton (2, 12, 26).

Although CagA translocation into host cells can potentiate IL-8 secretion (1, 6), the induction of proinflammatory cytokines has been shown to be mainly independent of CagA injection (10) but obviously requires a functional T4SS. Viala and colleagues identified T4SS-dependent peptidoglycan in the host cytoplasm interacting with intracellular nucleotide-binding oligomerization domain protein 1 (Nod1) via its internal caspase recruitment domain (CARD). Nod1 then activates nuclear factor kappa B (NF-κB), leading to transactivation of a wide range of proinflammatory cytokine and chemokines (30).

To obtain a better understanding of how *H. pylori* induces pathogenesis, many important studies were performed with cultured AGS or MKN-28 cells originating from individual human gastric adenocarcinomas. However, these cells differ considerably in their cellular responses to *H. pylori*. While *H. pylori*-infected AGS cells show rapid cell elongation within only a few hours, MKN-28 cells respond with a clear delay (23). Both cell lines secrete IL-8 in a *cag* PAI-dependent manner but to different extents (27), indicating differently regulated cell responses to *H. pylori*. This was underlined by another study

* Corresponding author. Mailing address: Division of Microbiology, Paris-Lodron University of Salzburg, Salzburg, Austria. Phone: 43 (0) 662 8044 7210. Fax: 43 (0) 662 8044 7209. E-mail: silja.wessler@sbg .ac.at.

TABLE 1. Mammalian gastric cell lines

Cell line	Source[a] (catalogue no.)	Growth properties	Origin, patient (age, yr)
AGS	ECACC (89090402)	Adherent	Adenocarcinoma, female (54)
MKN-1	JCRB (0252)	Adherent	Adenosquamous carcinoma, male (72)
MKN-7	JCRB (1025)	Adherent	Well-differentiated tubular adenocarcinoma, male (39)
MKN-28	JCRB (0253)	Adherent	Moderately differentiated tubular adenocarcinoma, female (70)
MKN-74	JCRB (0255)	Adherent	Liver metastasis from stomach cancer, male (37)
23123/87	DSMZ (ACC 201)	Adherent	Primary gastric adenocarcinoma, male (72)
Hs-746T	ATCC (HTB-135)	Adherent	Metastasis from gastric carcinoma in the left leg, male (74)
FU-97	JCRB (1074)	Adherent	Poorly differentiated adenocarcinoma, female (66)
MKN-45	JCRB (0254)	Adherent/suspension	Poorly differentiated adenocarcinoma, female (62)
Kato-3	JCRB (0611)	Suspension	Signet ring cell carcinoma, metastasis, male (55)
NUGC-4	JCRB (0834)	Suspension	Gastric lymph node, female (35)
SNU-1	ATCC (CRL-5971)	Suspension	Ascites of a poorly differentiated carcinoma, male (44)
SNU-5	ATCC (CRL-5973)	Suspension	Ascites of a poorly differentiated carcinoma, female (33)
SNU-16	ATCC (CRL-5974)	Suspension	Ascites of a poorly differentiated carcinoma, female (33)

[a] ATCC, American Type Culture Collection (www.atcc.org); DSMZ, Deutsche Sammlung von Mikroorganismen und Zellkulturen GmbH (www.dsmz.de); ECACC, European Collection of Cell Cultures (www.ecacc.org.uk); JCRB, Japanese Collection of Research Bioresources (http://cellbank.nibio.go.jp/).

demonstrating the involvement of several different host cell factors in 19 mammalian cell lines, of which only 4 were gastric epithelial cell lines (3).

However, there are more human gastric cell lines, which are still poorly characterized in regard to *H. pylori* infections. Here we performed a comparative study of 14 different gastric epithelial cell lines originating from human adenocarcinomas. We found remarkable differences in *H. pylori*-induced changes in cell morphology, adherence, CagA injection, vacuolization, and IL-8 synthesis. These data contribute to a broader insight into *H. pylori*-dependent cell responses and pathogenesis.

MATERIALS AND METHODS

Cell culture. 23123/87, AGS, MKN-1, MKN-7, MKN-28, MKN-45, MKN-74, and NUGC-4 cells (Table 1) were cultured in RPMI 1640 medium (Biochrom, Germany) with 4 mM L-glutamine (Invitrogen, Germany) and 10% fetal calf serum (FCS) (Biowest, France) in a humidified 5% CO_2 atmosphere at 37°C. Kato-3 cells grew in RPMI 1640 medium supplemented with 2 mM L-glutamine and 20% FCS. SNU-1 cells and SNU-16 cells were cultured in RPMI 1640 (Invitrogen, Germany) with 1.5 g/liter sodium bicarbonate, 1 mM sodium pyruvate, 2 mM L-glutamine, and 10% FCS. For the cultivation of Hs-746T cells, we used Dulbecco modified Eagle medium (DMEM) (Biochrom, Germany), 1 mM sodium pyruvate, 4 mM glutamine, and 10% FCS in a humidified 10% CO_2 atmosphere at 37°C. The cell line FU-97 was grown in DMEM supplemented with 1 mM sodium pyruvate, 4 mM glutamine, 10 mg/liter insulin (Invitrogen, Germany), and 10% FCS, and SNU-5 cells were cultured in Iscove modified Dulbecco medium (IMDM)-DMEM (1:1) (Biochrom, Germany) with 4 mM L-glutamine and 20% FCS. Adherent growing cells (AGS, MKN-1, MKN-7, MKN-28, MKN-74, 23123/87, Hs-746T, and FU-97 cells) (Table 1) were seeded in tissue culture plates at 48 h before infection and grown to subconfluence. At 2 h prior to infection, the medium was replaced by fresh medium containing 0.5% FCS. Suspension cells (MKN-45, Kato-3, NUGC-4, SNU-1, SNU-5, and SNU-16 cells) were centrifuged at 200 × *g* at 4°C for 10 min and counted, and 13.1 × 10^6 cells were seeded in cell culture flasks with medium containing 0.5% FCS at 2 h prior to infection.

Bacteria and infection experiments. *H. pylori* strains P12 (wild type; expressing Western CagA EPIYA-ABCC [23] and with a *vacA* s1/m1 genotype [25]), P12ΔPAI (31), and P12ΔVacA (25) have been described previously. *H. pylori* strains were cultured on agar plates containing 10% horse serum under microaerophilic conditions at 37°C for 48 h. For infection, bacteria were harvested in Dulbecco's phosphate-buffered saline (PBS) (pH 7.4) and added to the host cells at multiplicities of infection (MOIs) of 50 for 3, 6, 16, 24, 48, 72, and 96 h. As controls, PBS was incubated with the cells for the same time periods. During infection, cells were monitored using an inverse phase-contrast microscope (model TS 100; INTAS).

RNA isolation and real-time RT-PCR. Gastric epithelial cells were harvested at 0, 6, and 16 h poststimulation with *H. pylori* strains in RA1 buffer containing 1% β-mercaptoethanol. RNA isolation was performed as described in the Nucleo Spin RNAII kit protocol (Macherey-Nagel, Germany). Using the RevertAid H Minus first-strand cDNA synthesis kit (Fermentas, Germany) with random primers according to the kit protocol, 2 μg mRNA was transcribed into cDNA. Oligonucleotide primers and probes specific for the 16S rRNA gene (forward, 5′-AGC CAT AGG ATT TCA CAC CTG AC-3′; reverse, 5′-GCA AGC GTT ACT CGG AAT CAC-3′; probe, 5′-FAM-CCC GCC TAC ACG CTC TTT ACG CCC-TAMRA-3′) and the glyceraldehyde-3-phosphate dehydrogenase (GAPDH) housekeeping gene (forward, 5′-CCT GCA CCA CCA ACT GCT TA-3′; reverse, 5′-CAT GAG TCC TTC CAC GAT ACC A-3′; probe, 5′-FAM-CCT GGC CAA GGT CAT CCA T-TAMRA-3′) were used in real-time reverse transcription-PCR (RT-PCR) (Rotor-Gene 6000, Qiagen). For amplification, the Maxima Probe qPCR Master-Mix (Fermentas) was used according to manufacturer's instructions. Each PCR cycle consisted of a denaturation step (94°C, 30 s), an annealing step (60°C, 30 s), and an elongation step (72°C, 30 s). All data were normalized with the corresponding GAPDH transcription level using a comparative Δ*CT* method.

Neutral red-based assay. To measure cell vacuolization, $1 × 10^4$ adherent cells per well were seeded in 96-well plates and cultivated for 24 h. Prior to infection, the medium of adherent cells was replaced by medium containing 0.5% FCS. A total of $1.5 × 10^4$ suspension cells per well were seeded in 96-well plates for 2 h. Both adherent and suspension cells were infected with wild-type or ΔVacA mutant *H. pylori* at an MOI 50 for 24 h. The neutral red-based assay (Sigma-Aldrich, Germany) was performed according to the manufacturer's recommendations. The neutral red solution was incubated with the cells (1:10) at 37°C for 2 h. The medium was carefully removed and the cells quickly rinsed with neutral red assay fixative. The incorporated dye was then solubilized in neutral red assay solubilization solution, and the absorbance at 560 nm was recorded using a microplate reader (Tecan, Germany).

MTT viability assay. To measure the cell viability in an assay with 3-(4,5-dimethylthiazol-2-yl)-2,5-diphenyltetrazolium bromide (MTT), $1 × 10^4$ adherent cells per well were seeded in 96-well plates and cultivated for 24 h. Prior to infection, the medium of adherent cells was replaced by medium containing 0.5% FCS. A total of $1.5 × 10^4$ of suspension cells per well were seeded in 96-well plates for 2 h. Both adherent and suspension cells were infected with *H. pylori* at an MOI of 50 for 24 and 96 h. The colorimetric cell survival and proliferation assay (Millipore, Germany) was performed according to the manufacturer's recommendations, with minor alterations. Briefly, plates were incubated at 37°C for 1 h, and then the assay was stopped by adding color development solution and absorbance at 560 nm was recorded using a microplate reader (Tecan, Germany).

Immunoprecipitation, SDS-PAGE, and immunoblotting. Cells were washed twice with PBS, harvested in lysis buffer (20 mM Tris–HCl [pH 7.5], 1 mM ETDA, 100 mM NaCl, 1% Triton X-100, 0.5% sodium deoxycholate, 0.1% SDS, 1× complete protease inhibitors [Roche, Germany], 1 mM Na_3VO_4, 1 mM sodium molybdate, 20 mM NaF, 10 mM sodium pyrophosphate, 20 mM β-glycerophosphate), and separated by SDS-PAGE. Suspension cells were additionally

centrifuged at 200 × g at 4°C for 10 min after each washing step and finally harvested in lysis buffer. Proteins were transferred onto nitrocellulose membranes, blocked with Odyssey blocking buffer (Li-Cor Biosciences, Germany), and probed with anti-pY99 (Santa Cruz, Germany) to detect tyrosine-phosphorylated CagA, with anti-CagA (IBT, Germany) to detect CagA, or with anti-GAPDH (Abcam, United Kingdom) for GAPDH detection. The expression of the non-receptor tyrosine kinases c-Abl and Src was determined using specific anti-Abl antibody (24-11, sc-23; Santa Cruz, Germany) or anti-Src antibody (sc-18, which detects c-Src, Yes p62, Fyn p59, c-Fgr p55, and c-Src 2; Santa Cruz, Germany). To analyze and quantify CagA tyrosine phosphorylation, CagA was immunoprecipitated using a polyclonal CagA antibody (IBT, Germany), and tyrosine phosphorylation was detected using an anti-phosphotyrosine antibody (pY99; Santa Cruz). Membranes were analyzed with an Odyssey 2.1 instrument (Li-Cor Biosciences, Germany) by using anti-mouse IRDye 800 and anti-rabbit IRDye 680 secondary antibodies (Li-Cor Biosciences, Germany).

IL-8 ELISA. Determination of interleukin-8 (IL-8) release was performed using an IL-8-specific enzyme-linked immunosorbent assay (ELISA) system (Biolegend). After cells were colonized with wild-type *H. pylori* and an *H. pylori* ΔPAI mutant or left untreated, supernatants were collected and centrifuged. Aliquots of supernatants were analyzed for IL-8 release as recommend by the manufacturer.

Statistical analysis. All data were evaluated using Student t test. P values of <0.001 (∗∗∗), <0.01 (∗∗), and <0.05 (∗) were considered statistically significant.

RESULTS

Cell morphological response to *H. pylori*. We investigated cellular responses to *H. pylori* in 14 different gastric carcinoma cell lines by colonizing AGS, MKN-1, MKN-7, MKN-28, MKN-74, 23123/87, Hs-746T, FU-97, MKN-45, Kato-3, NUGC-4, SNU-1, SNU-5, and SNU-16 cells (Table 1) with *H. pylori* at an MOI of 50 for different time periods and monitoring changes in cellular phenotype, such as cellular elongation, cell (dis)aggregation, and vacuolization. Data obtained from experiments with adherent AGS, MKN-1, MKN-7, MKN-28, MKN-74, 23132/87, Hs-746T, and FU-97 cells are shown in Fig. 1A. AGS cells were seeded into tissue plates to form cell colonies exhibiting the typical round epithelial cell morphology. *H. pylori* induced strong AGS cell scattering as adherent cell colonies completely dispersed; cells lost cell-to-cell contacts and became highly elongated. As expected, this phenotype was fully developed after 24 and 48 h (Fig. 1A). Compared to AGS cells, colonies formed by MKN-28 cells did not totally disseminate upon *H. pylori* infection. Only a few cells of the MKN-28 colonies had elongated after 24 h and proceeded further after 48 h (Fig. 1A). Noninfected MKN-1 cells already exhibited a slightly elongated phenotype, which became more pronounced after infection with *H. pylori*, comparable to that for Hs-746T cells (Fig. 1A). In contrast, MKN-74 cells only marginally changed their cellular morphology in response to *H. pylori* infection (Fig. 1A). Even after 96 h, MKN-74 cells maintained round cell morphology and cellular adhesion. Comparable to MKN-74 cells, MKN-7, 23123/87, and FU-97 cells did not elongate (Table 2; Fig. 1A). These data indicate that adherent cells respond differentially to *H. pylori* infection.

Analyzing gastric suspension cells, we observed that noninfected Kato-3 cells formed small homotypic cell aggregates. Upon *H. pylori* infection for 24 h, cell aggregates clearly enlarged (Fig. 1B), suggesting that *H. pylori* might induce the expression of cell adhesion proteins, which has been already shown for aggregating U937 cells (17). In contrast to the *H. pylori*-dependent phenotype of Kato-3 cells, NUGC-4 and SNU-1 cells disaggregated upon *H. pylori* infection (Fig. 1B). Noninfected NUGC-4 and SNU-1 cells both grew in large

coherent aggregates whose size decreased after 24 and 48 h of infection with *H. pylori* (Fig. 1B). Similar data were obtained with SNU-5 and SNU-16 cells (Table 2; Fig. 1B). MKN-45 cells grow as both spindle-shaped cells in monolayers and single rounded cells or clumps in suspension. However, in response to *H. pylori*, MKN-45 cells did not change their morphology (Fig. 1B). The results of detailed analyses of all 14 tested cell lines are summarized in Table 2. For example, comparing the extents of cell elongation or morphology, the typical characteristics of group "++" are the complete loss of cell-to-cell adhesions and strong cellular elongation comparable to that for AGS cells, whereas only partially elongated cells were included in group "+" (e.g., MKN-28 cells). *H. pylori*-infected cell lines that did not change their cell morphology were classified as "0" (e.g., MKN-74 cells). Suspended cells were rated in terms of cellular aggregation or disaggregation as indicated (Table 2).

***H. pylori* adherence to host cells.** The effects that we observed might be caused by different loads of adherent *H. pylori* in the individual tested cell lines. Since the conventional determination of CFU is highly fault prone and cannot exactly be correlated to the amounts of different host cells, we quantified the loads of bacteria and host cells by 16S rRNA and GAPDH gene amplification, respectively, via real-time PCR, detecting both attached and internalized bacteria. After infection with *H. pylori* for 6 h and 16 h at an MOI of 50, total RNA originating from *H. pylori* and host cells was prepared and the relative amounts of 16S rRNA and GAPDH genes were quantified by quantitative PCR (qPCR) (Fig. 2). A 16S rRNA/GAPDH gene ratio of 88.4 was determined for AGS cells after *H. pylori* infection for 6 h (Fig. 2, black bars), which was further increased after 16 h of infection (ratio of 270.8) (Table 2; Fig. 2, gray bars). Compared to binding to AGS cells, *H. pylori* showed a significantly increased binding to MKN-7 cells and equal binding to MKN-1, MKN-28, 23123/87, Hs-746T, FU-97, MKN-45, NUGC-4, SNU-1, and SNU-16 cells after 6 h. Less *H. pylori* adherence was detected using MKN-74, Kato-3, and SNU-5 cells (Fig. 2, black bars). In comparison to AGS cells which were infected for 16 h, significantly more *H. pylori* adhered to MKN-7 cells, and significantly fewer bacteria interacted with MKN-1, MKN-74, Hs-746T, MKN-45, Kato-3, NUGC-4, SNU-5, and SNU-16 cells. However, adherence to MKN-28, 23123/87, and SNU-1 cells was similar to that to AGS cells (Fig. 2, gray bars). In summary, we concluded that compared to noninfected cells (ratio of <0.01), *H. pylori* adhered to all tested cell lines with different affinities (Table 2).

Extent of VacA-induced vacuolization. Virulent *H. pylori* strains secrete VacA, a multifunctional pathogenic factor that induces large vacuoles in epithelial cells (24). Hence, we also analyzed the gastric epithelial cells for VacA-dependent vacuolization. All the cells were infected with wild-type *H. pylori* or the isogenic VacA deletion mutant for 24 h. Compared to the results for noninfected cells, wild-type *H. pylori* did not induce enhanced vacuolization in SNU-1 and AGS cells, which has been previously reported for AGS cells (29). Interestingly, strong vacuolization was observed in MKN-1, MKN-28, MKN-74, FU-97, and MKN-45 cells, which was significantly reduced after infection with the VacA deletion mutant (Fig. 3A; Table 2). MKN-7, 23123/87, Hs-746T, Kato-3, and NUGC-4 cells showed a moderate VacA-dependent vacuolization, while vac-
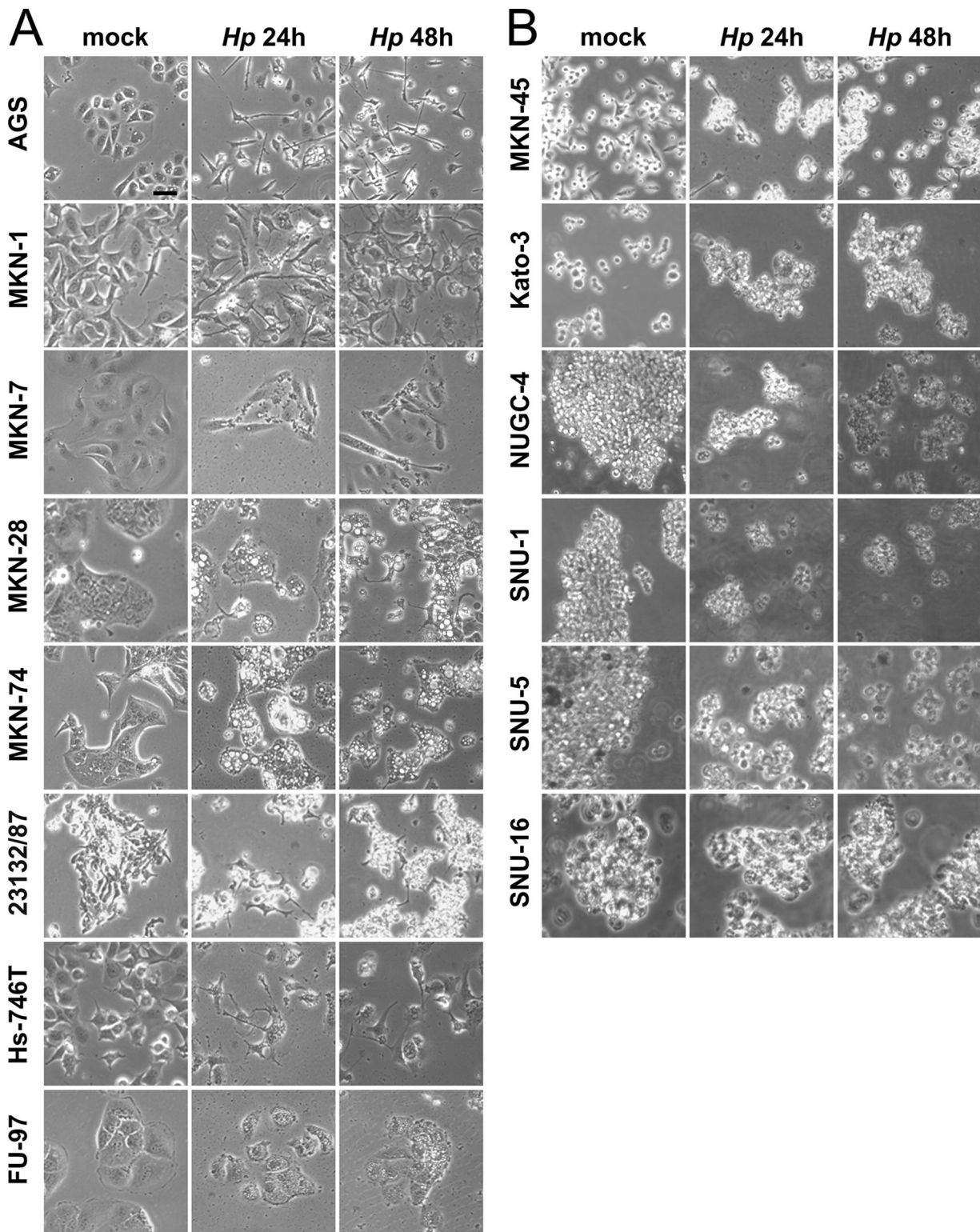
FIG. 1. Characteristic phenotypes of gastric epithelial cells after *H. pylori* (*Hp*) infection. Adherent cells (AGS, MKN-1, MKN-7, MKN-28, MKN-74, 23132/87, Hs-746T, and FU-97 cells) (A) and suspension cells (MKN-45, Kato-3, NUGC-4, SNU-1, SNU-5, SNU-16 cells) (B) were infected with *H. pylori* at an MOI of 50. After 24 and 48 h, cells were visualized by phase-contrast microscopy and compared to noninfected cells (mock infection after 48 h). The results are representative of four independent experiments. Scale bar, 25 μm.

TABLE 2. Cellular responses to *H. pylori* infection

Cell line	Adherence (mean ± SE)[a]	Cell elongation[b]	CagA phosphorylation[c]	Vacuolization[d]	IL-8 secretion at 24 h (pg/ml, mean ± SE)	
					Mock infection	*H. pylori* infection
AGS	270.8 ± 9.4	++	++	0	440 ± 170	5,658 ± 1,616
MKN-1	49.5 ± 5.8	+	+	++	3,934 ± 3,649	40,060 ± 278
MKN-7	441.9 ± 26.0	0	+	+	608 ± 708	23,928 ± 2,862
MKN-28	356.8 ± 64.3	+	+	++	688 ± 39	6,020 ± 269
MKN-74	19.6 ± 3.7	0	+	++	39 ± 36	1,335 ± 474
23123/87	485.5 ± 140.6	0	++	+	10,566 ± 3,691	65,638 ± 5,601
Hs-746T	37.2 ± 20.8	+	++	+	54 ± 47	6,294 ± 195
FU-97	138.9 ± 38.4	0	+	++	22 ± 26	59 ± 56
MKN-45	53.4 ± 3.8	0	+++	++	219 ± 63	11,682 ± 2,710
Kato-3	39.4 ± 19.0	Aggregation	+++	+	916 ± 725	7,359 ± 4,541
NUGC-4	62.2 ± 19.4	Disaggregation	++	+	357 ± 239	5,702 ± 5,685
SNU-1	153.8 ± 70.6	Disaggregation	+	0	11 ± 1	20 ± 5
SNU-5	36.6 ± 4.2	Disaggregation	++	0	198 ± 208	979 ± 1,000
SNU-16	62.9 ± 35.4	Disaggregation	+	0	20 ± 8	797 ± 512

[a] Adherence was rated according to the 16S rRNA/GAPDH gene ratio after infection with *H. pylori* for 16 h (ratio for noninfected cells, < 0.01).
[b] Cell elongation was compared to the strong cellular elongation seen with AGS cells (++). +, partially elongated cells; 0, cell lines that did not change morphology. Suspended cells were rated in terms of cellular aggregation or disaggregation.
[c] CagA phosphorylation intensity was quantified in relation to CagA intensity detected in Western blot analyses. +++, phospho-CagA/CagA ratio of >40%; ++, phospho-CagA/CagA ratio of <40%; +, phospho-CagA/CagA ratio of <15%.
[d] Vacuolization in adherent cells was rated according to the fold induction of vacuolization in a neutral red assay as shown in Fig. 3 (++, fold induction of >1.5; +, fold induction of >1; 0, fold induction of <1).

uolization in SNU-5 and SNU-16 cells was reduced (Fig. 3A; Table 2).

To investigate the possibility that the observed effects are influenced by alteration of cell survival, we performed MTT assays to monitor the cellular viability and proliferation. Compared to the results for mock-infected cells after 24 h, *H. pylori* did not induce obvious alterations in cell viabilities during the early phases of infection. Unsurprisingly, the amounts of vital cells after 96 h for some cell lines (such as MKN-1, MKN-28, MKN-74, MKN-45, Kato-3, NUGC-4, and SNU-1) were increased compared to those for mock-infected cells after 24 h,
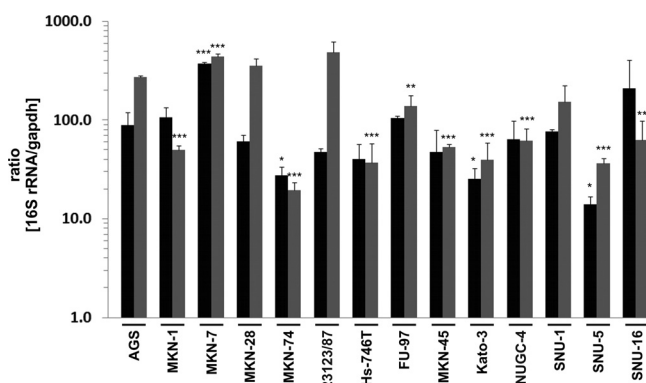

FIG. 2. *H. pylori* adherence to gastric epithelial cells. Adherence of *H. pylori* to different cell lines was investigated by real-time PCR analysis. The 16S rRNA gene from adherent and internalized *H. pylori* and the host GAPDH gene were amplified from cells infected for 6 h (black bars) and 16 h (gray bars), and the results are presented as the 16S rRNA/GAPDH gene ratio for *H. pylori*-infected cells. Data are presented as the mean values with standard errors from two independent experiments with two replications. Asterisks indicate statistically significant differences of the 16S rRNA/GAPDH ratio for *H. pylori*-infected cells compared to AGS cells after the corresponding infection period (*, $P < 0.05$; **, $P < 0.01$; ***, $P < 0.001$).

which were affected by infection with *H. pylori* after infection for 96 h (Fig. 3B).

Translocation of *H. pylori* CagA. It has been suggested that *H. pylori* interferes with components of the actin cytoskeleton and focal adhesions of epithelial cells, resulting in drastic cell elongation *in vitro* and in neoplastic transformation *in vivo*. These effects were attributed to tyrosine-phosphorylated CagA acting as a crucial signaling molecule in host cells (2). In transfected cells expressing exogenous CagA, it was also demonstrated that the extent of cell elongation depends on the number and sequences of tyrosine phosphorylation sites (13). Hence, we investigated CagA phosphorylation in 14 gastric epithelial cell lines. CagA was immunoprecipitated from lysates of cells infected with *H. pylori* for 6 h, and phospho-CagA was detected in immunocomplexes by Western blot analyses. Signal intensities were quantified in relation to CagA and either plotted on a bar chart or expressed as "+" values for the phospho-CagA/CagA ratio (Fig. 4A; Table 2). Unexpectedly, we found the strongest phosphorylation of CagA in MKN-45 and Kato-3 cells, while CagA was clearly tyrosine phosphorylated in AGS, 23123/87, NUGC-4, and SNU-5 cells. A low CagA phosphorylation intensity was detected in MKN-1, MKN-7, MKN-28, MKN-74, Hs-746T, FU-97, SNU-1, and SNU-16 cells (Fig. 4A). These data show that CagA phosphorylation strongly differs in epithelial cells. The extent of CagA phosphorylation might be caused by the differentially expressed CagA kinases of the Src and Abl families. Analyzing kinase expression, equal amounts of proteins were separated by SDS-PAGE and kinases were detected by Western blotting (Fig. 4B). c-Abl was strongly expressed in Kato-3, MKN-7, MKN-74, SNU-1, and NUGC-4 cells, and the lowest c-Abl level was observed in AGS cells. Src family kinases (SFK) were detected using an antibody recognizing c-Src p60, Yes p62, Fyn p59, c-Fgr p55, and c-Src 2, which have different molecular weights. The profile of SFK expression shows a differential
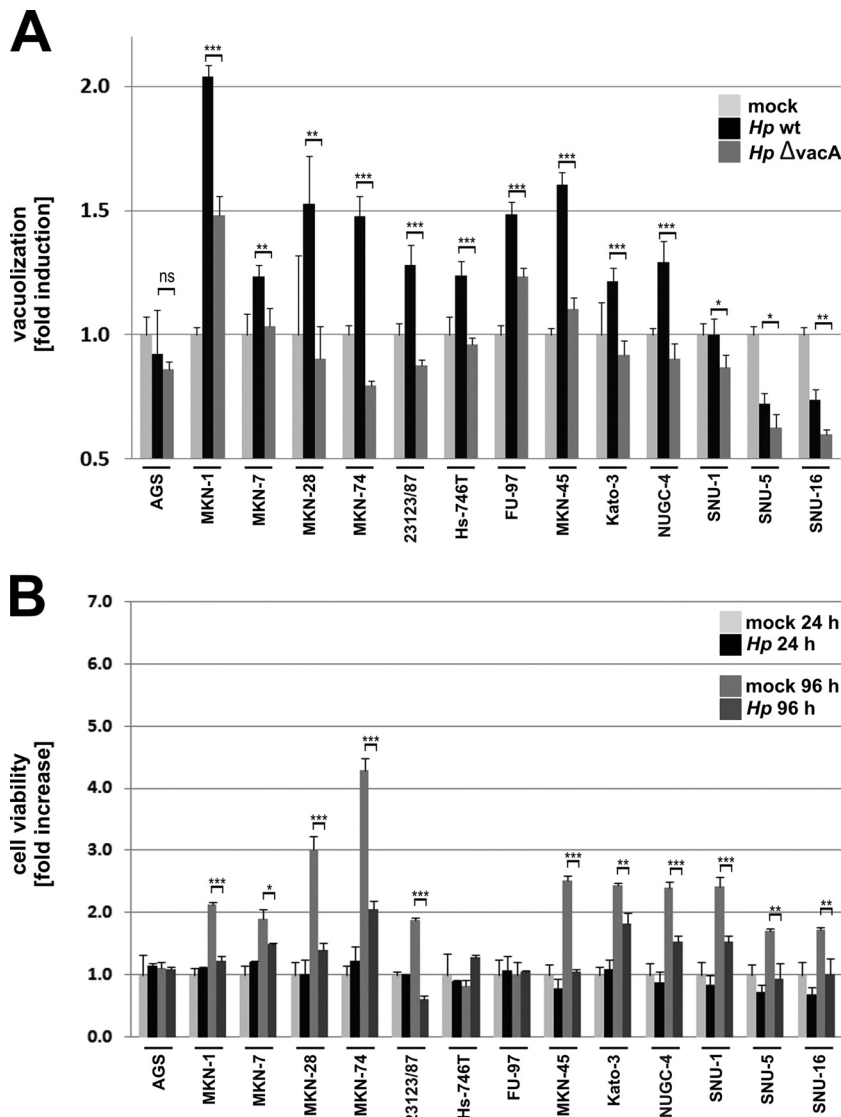
FIG. 3. Quantification of *H. pylori*-dependent vacuolization and cell viability. (A) Cells were infected with wild-type *H. pylori* (wt) or an isogenic ΔVacA mutant. The vacuolization was determined in a neutral red assay, and the results are expressed as fold induction against noninfected cells from each cell line (set as 1). Data are presented as the mean values with standard errors from two independent experiments with four replications. Asterisks indicate statistically significant differences between wild-type *H. pylori*- and ΔVacA mutant-induced vacuolization (*, $P < 0.05$; **, $P < 0.01$; ***, $P < 0.001$). (B) Cell viability was analyzed after infection with *H. pylori* for 24 h and 96 h in an MTT assay. The results indicate the fold increase of cell viability in response to *H. pylori* and are compared to results for noninfected cells after 24 h and 96 h. Data are presented as the mean values with standard errors from two independent experiments with three replications. Asterisks indicate statistically significant differences in viability of mock-treated and *H. pylori*-infected cells (*, $P < 0.05$; **, $P < 0.01$; ***, $P < 0.001$).

expression pattern in the tested cell lines (Fig. 4B), which might influence the extent of CagA phosphorylation.

Since we observed differences in the phosphorylation intensity, we further considered the kinetics of CagA tyrosine phosphorylation (Fig. 5). A phospho-CagA signal was detected in AGS and MKN-74 cells, which rapidly increased within the early phase of *H. pylori* infection and then remained relatively constant. Similar but attenuated kinetics were shown in MKN-1, MKN-7, Hs-746T, and FU-97 cells. CagA and GAPDH detection served as controls (Fig. 5). A different type of CagA phosphorylation kinetics was observed in NUGC-4, MKN-45, and SNU-5 cells. Here, CagA phosphorylation decreased again

after 48 h (Fig. 5). The decrease in CagA phosphorylation was more pronounced in MKN-28, 23123/87, Kato-3, SNU-1, and SNU-16 cells, where phospho-CagA increased rapidly but decreased again at 24 h postinfection (Fig. 5).

***H. pylori*-induced IL-8 secretion.** The induction of proinflammatory cytokines and chemokines was shown to be dependent on a functional T4SS (10, 27). In a previous study, considerable differences in IL-8 secretion in different mammalian cells were observed (3). Hence, we also investigated the *H. pylori*-induced release of IL-8 into culture medium of human gastric epithelial cells. To compare the cell type-specific range of IL-8 secretion of the tested cell lines (Fig. 6), IL-8 secretion
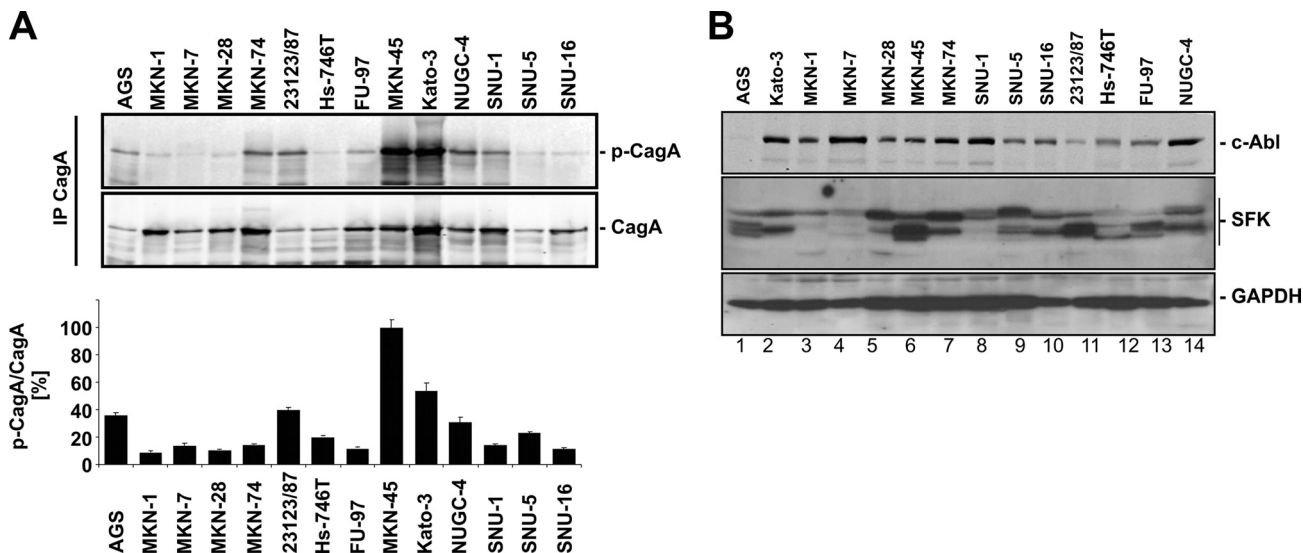
FIG. 4. Tyrosine phosphorylation of bacterial CagA by host cell family kinases during *H. pylori* infection. (A) CagA was immunoprecipitated from 200 μg of protein lysates of cells infected with *H. pylori* for 6 h. Tyrosine-phosphorylated CagA in the immunocomplex was detected by immunoblotting using a phospho-specific tyrosine antibody, and results are presented as a representative blot (upper panel). Phosphorylated CagA and CagA were quantified, and data were calculated as the phospho-CagA/CagA ratio from at least three independent experiments and are presented as the means ± standard deviations in a bar chart; phospho-CagA/CagA ratios obtained from MKN-45 cells were set as 100% (lower panel). (B) Proteins (100 μg) were separated by SDS-PAGE and blotted onto membranes. c-Abl and SFKs were detected using specific antibodies, and representative data are shown. GADPH was used to monitor cellular expression levels.
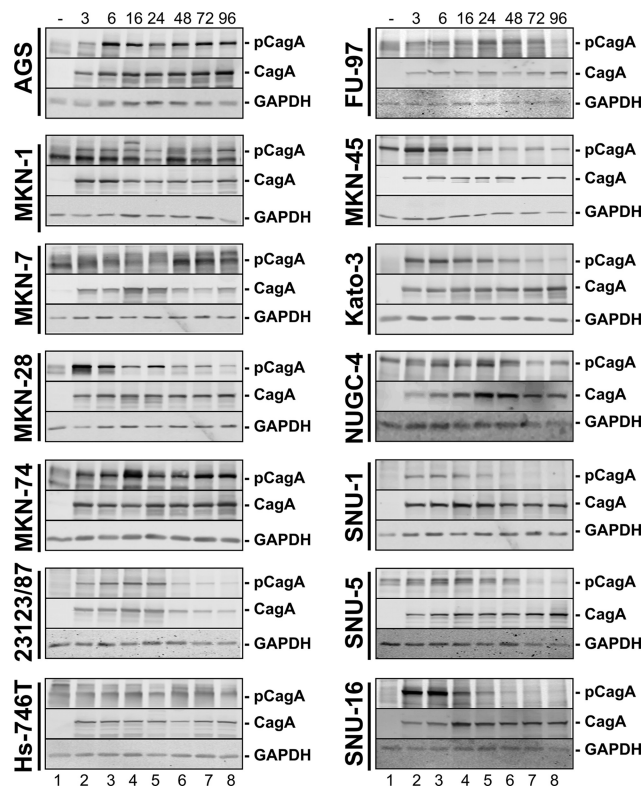

FIG. 5. Kinetics of CagA phosphorylation. Cells were either left untreated (−) or infected with *H. pylori* at an MOI of 50 for the indicated time periods. CagA tyrosine phosphorylation was analyzed by immunoblotting using an anti-phosphotyrosine (p-CagA) or anti-CagA antibody. GAPDH was detected as a loading control. Note that MKN-1, MKN-7, NUGC-4, and MKN-45 cells (lanes 1) express proteins with slightly different molecular weights compared to CagA detected by the anti-phosphotyrosine antibody. Representative data from two independent experiments are shown.

after 24 h in *H. pylori*- and mock-infected cells is summarized in Table 2. The results indicate cell type-specific cytokine responses in *H. pylori*-colonized human gastric epithelial cells varying between 20 pg/ml (SNU-1 cells) and approximately 65×10^3 pg/ml IL-8 (23123/87 cells) (Table 2). Furthermore, the *H. pylori*-mediated induction of IL-8 varied from 2-fold (SNU-1 cells) to approximately 53-fold (MKN-45 cells) and 116-fold (Hs-746T cells) (Table 2). As expected, the *H. pylori*-induced IL-8 secretion was strongly dependent on a functional type IV secretion system encoded by the *cag* PAI (Fig. 6C). Finally, the kinetics were significantly different. AGS and MKN-28 cells showed strong induction within 3 to 6 h after infection with *H. pylori*. IL-8 further increased within 24 h and then reached a plateau of approximately 14,000 or 7,000 pg/ml (Fig. 6A). Similar kinetics were obtained with infected 23123/87 and MKN-45 cells (Fig. 6A and B). However, *H. pylori*-infected MKN-74 cells responded with different IL-8 secretion kinetics. Small amounts of IL-8 were detected at 3 h after *H. pylori* infection, and these steadily increased during infection without reaching a plateau (Fig. 6A), which was also found after infection of MKN-1, MKN-7, FU-97, and Hs-746T cells (Fig. 6A). In contrast, NUGC-4 and Kato-3 cells showed an increase in IL-8 secretion with a peak after 16 and 24 h, respectively. Prolonged infection with *H. pylori* led to a decline in IL-8 synthesis as detected in SNU-5 and SNU-16 cells (Fig. 6B). Finally, IL-8 in SNU-1 cells was only marginally induced (Fig. 6B), which did not correlate with the *H. pylori*-induced IL-8 release in SNU-5 or SNU-16 cells (Table 2; Fig. 6B).

In summary, these data show that *H. pylori* induced cell line-specific responses, indicating that different host factors are involved in the induction of cell elongation, vacuolization, CagA phosphorylation, and cytokine release.
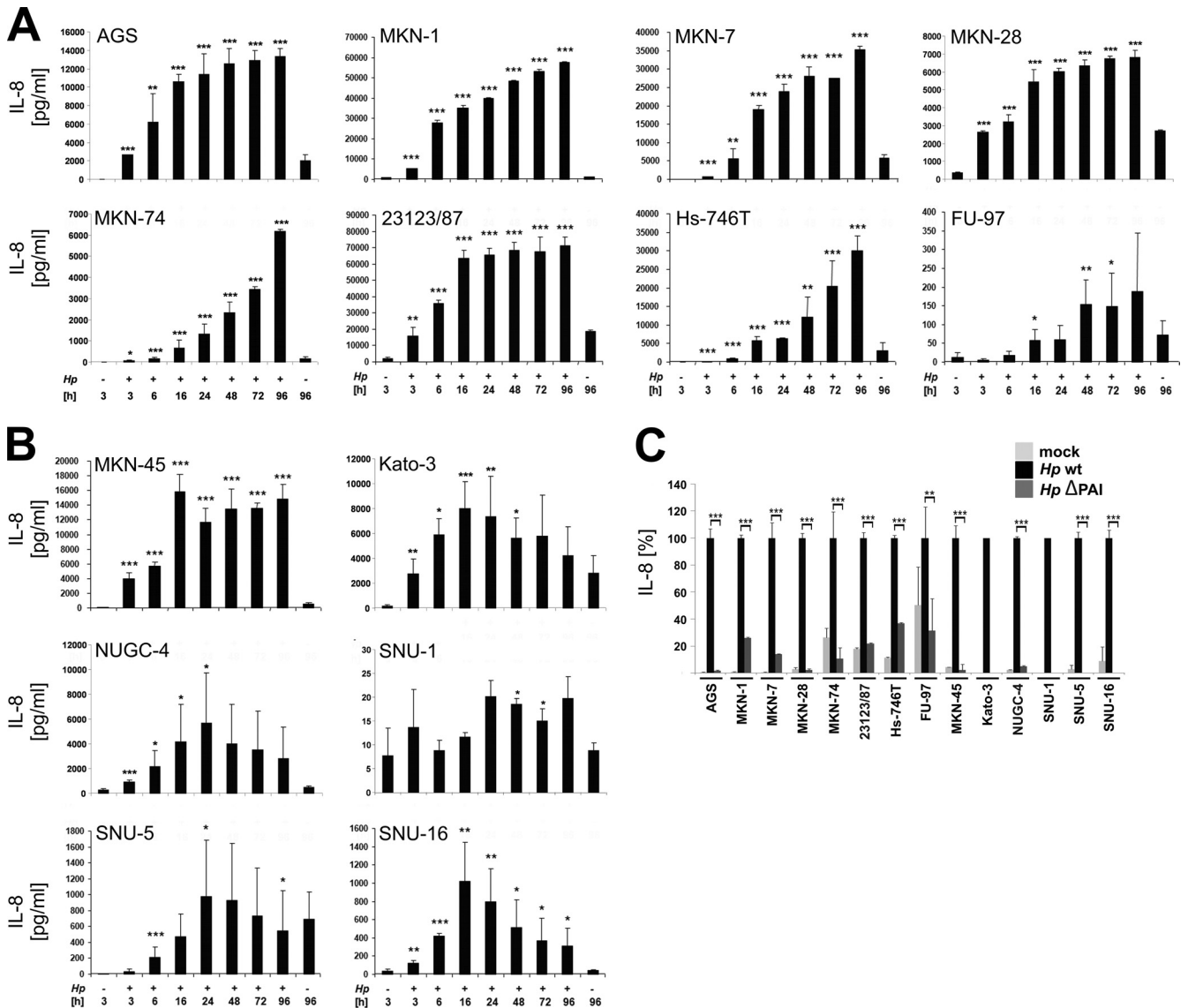
FIG. 6. IL-8 secretion by *H. pylori*-infected gastric epithelial cells. (A and B) All adherent cells (A) and cells in suspension (B) were either left untreated (−) or infected with *H. pylori* at an MOI of 50 for 96 h. IL-8 secretion was determined by ELISAs, comparing each time point with its corresponding noninfected control. Only the controls of noninfected cells after 3 h and 96 h are shown. Data are presented as the mean values with standard errors from four independent experiments with three replications. Asterisks indicate statistically significant differences between *H. pylori*-induced IL-8 secretion after a given time point and its corresponding mock-infected control (∗, $P < 0.05$; ∗∗, $P < 0.01$; ∗∗∗, $P < 0.001$). (C) Cells were infected with wild-type *H. pylori* or its isogenic ΔPAI mutant at an MOI of 50 for 24 h or were left untreated. Aliquots of supernatants were analyzed for IL-8 secretion. The amounts of IL-8 after wild-type *H. pylori* infection were set 100%. Data are presented as the mean values with standard errors from two independent experiments with three replications. Asterisks indicate statistically significant differences between wild-type and ΔPAI *H. pylori*-induced IL-8 secretion (∗, $P < 0.05$; ∗∗, $P < 0.01$; ∗∗∗, $P < 0.001$).

DISCUSSION

Helicobacter pylori persistently colonizes the human gastric mucosa and is associated with the development of gastritis, duodenal and peptic ulcers, gastric adenocarcinoma, and MALT lymphoma (8, 18, 21). Neoplastic transformation has been strongly associated with the translocated effector protein CagA of *H. pylori*. In fact, a direct causal link between CagA and *in vivo* oncogenesis was demonstrated in transgenic mice expressing CagA, which developed gastric polyps and adenocarcinomas of the stomach and small intestine (19). *In vitro*, *H. pylori* injects CagA through a T4SS, followed by tyrosine

phosphorylation and deregulation of host signaling proteins, which might contribute to the malignancy of gastric tumors.

The overwhelming majority of these important findings were obtained from well-established and characterized *in vitro* model systems for human adenocarcinoma of the stomach (e.g., AGS or MKN-28 cells). These cells were isolated from different patients with individual clinical histories (Table 1). Correspondingly, these studies also indicate cell type-specific signaling mechanisms and responses induced by *H. pylori* (3). During neoplasia and cancer progression, cells transform and dedifferentiate due to "loss-of-function" or "gain-of-func-

tion" mutations (32) leading to a protein expression pattern different from that of primary cells. Therefore, in the present study we compared 14 different immortalized gastric cell lines originating from patients with adenocarcinoma of the stomach (Table 1) and found that the tested cell lines respond to *H. pylori* with clearly different, pronounced characteristics.

The current model of *H. pylori*-dependent cytoskeletal rearrangements leading to host cell scattering and elongation points to components of the T4SS binding to β1-integrins on epithelial host cells, allowing CagA injection and phosphorylation (15, 16). Using 14 different gastric cell lines, we observed clear differences in CagA phosphorylation intensities and kinetics. Previously, we showed that CagA is initially phosphorylated by Src family kinases, which are replaced by Abl kinases, allowing sustained CagA phosphorylation in prolonged *H. pylori* infections (23, 28). Here, we found that CagA was steadily phosphorylated in AGS cells, while phospho-CagA decreased again after prolonged *H. pylori* infection in NUGC-4, Kato-3, or SNU-1 cells, suggesting that Src and Abl kinases might be either differentially expressed or activated. In fact, we found different expression levels of c-Abl and Src kinases. In addition to CagA phosphorylation kinetics, we also observed different intensities of cytoplasmic CagA phosphorylation, based on normalization to total CagA. We assume that these data are the result of different kinase activities together with differences in CagA translocation and with bacterial adherence determining the extent of CagA phosphorylation.

Phosphorylated CagA activates distinct signaling pathways that target the actin cytoskeletal rearrangements involved in host cell scattering and elongation (26). In transfection studies, it was also indicated that the number and sequence of CagA tyrosine phosphorylation sites determine the elongation of adherent cells (13). Interestingly, we observed additional parameters influencing the CagA-induced alteration of cell morphology. For instance, 23123/87 and Hs-746T cells showed strong CagA phosphorylation but obviously less elongation than AGS cells (Table 2). A plausible explanation is provided by recent findings that VacA and CagA have antagonistic functions (20, 29). Tegtmeyer and colleagues demonstrated that a VacA-mediated membrane signaling pathway inhibited CagA-mediated cell elongation independently of its vacuolization activity. Downregulation of the VacA receptor RPTPα restored CagA-dependent cell elongation (29). Accordingly, we found a correlation between weak vacuolization and strong CagA phosphorylation (Table 2), supporting the previous findings that active VacA is a crucial factor in CagA phosphorylation. Corresponding to the observation that VacA inhibited CagA-dependent processes, others postulated that in turn, CagA blocked VacA-dependent processes (20), underlining the complex interfering functions of CagA and VacA.

In macrophage-like cells, *H. pylori* induced upregulation of intracellular adhesion molecule 1 (ICAM-1), leading to the formation of large homotypic aggregates (3, 17). ICAM-1 is an intercellular adhesion molecule, present mainly in leukocytes and endothelial cells but also expressed in Kato-3 cells (14). We observed the formation of large cell aggregates upon infection with *H. pylori* in these cells, suggesting induced expression of intercellular adhesion molecules, such as ICAM-1. This effect was interesting, since in response to *H. pylori* we found that other cell lines grown in suspension disaggregated instead,

implying complex cell type-specific mechanisms of *H. pylori*-colonized cells.

Chronic inflammation of the persistently *H. pylori*-infected mucosa contributes to neoplastic transformation (7). *H. pylori* induces the synthesis of a broad range of proinflammatory cytokines and chemokines in gastric epithelial cells in a T4SS-dependent, but CagA-independent, manner (9, 10). Hence, we also analyzed secretion of IL-8 upon infection in all tested cell lines and found that the induction of IL-8 differed greatly (Table 2). This strongly argues for additional host cell-specific factors and against impaired *H. pylori* colonization of these cell lines as the limiting factor. A low *H. pylori* colonization was detected for Hs-746T, MKN-74, Kato-3, and SNU-5 cells; however, those cells showed IL-8 secretion levels from moderate to strong (Table 2). This is underlined by the finding that cells which are highly bound by *H. pylori* (e.g., 23123/87 or MKN-7 cells) did not strongly elongate and showed moderate CagA phosphorylation (Table 2). These data support our hypothesis of a complex interaction of host cell-specific and bacterial factors that determines cellular responses to *H. pylori*.

In summary, we performed a comprehensive and comparative analysis of different cellular responses of *H. pylori*-infected cells. Comparing 14 gastric cell lines revealed differentially regulated processes, indicating the importance of gaining deeper knowledge about the cell lines used in investigating *H. pylori* pathogenesis.

REFERENCES

1. **Argent, R. H., J. L. Hale, E. M. El-Omar, and J. C. Atherton.** 2008. Differences in *Helicobacter pylori* CagA tyrosine phosphorylation motif patterns between western and East Asian strains, and influences on interleukin-8 secretion. J. Med. Microbiol. **57:**1062–1067.
2. **Backert, S., S. M. Feller, and S. Wessler.** 2008. Emerging roles of Abl family tyrosine kinases in microbial pathogenesis. Trends Biochem. Sci. **33:**80–90.
3. **Bauer, B., S. Moese, S. Bartfeld, T. F. Meyer, and M. Selbach.** 2005. Analysis of cell type-specific responses mediated by the type IV secretion system of *Helicobacter pylori*. Infect. Immun. **73:**4643–4652.
4. **Blaser, M. J., and J. C. Atherton.** 2004. *Helicobacter pylori* persistence: biology and disease. J. Clin. Invest. **113:**321–333.
5. **Bodger, K., and J. E. Crabtree.** 1998. *Helicobacter pylori* and gastric inflammation. Br. Med. Bull. **54:**139–150.
6. **Brandt, S., T. Kwok, R. Hartig, W. Konig, and S. Backert.** 2005. NF-kappaB activation and potentiation of proinflammatory responses by the *Helicobacter pylori* CagA protein. Proc. Natl. Acad. Sci. U. S. A. **102:**9300–9305.
7. **Correa, P.** 2004. The biological model of gastric carcinogenesis. IARC Sci. Publ. **2004:**301–310.
8. **Cover, T. L., and M. J. Blaser.** 1992. *Helicobacter pylori* and gastroduodenal disease. Annu. Rev. Med. **43:**135–145.
9. **Crabtree, J. E., and S. M. Farmery.** 1995. *Helicobacter pylori* and gastric mucosal cytokines: evidence that CagA-positive strains are more virulent. Lab. Invest. **73:**742–745.
10. **Fischer, W., et al.** 2001. Systematic mutagenesis of the *Helicobacter pylori* cag pathogenicity island: essential genes for CagA translocation in host cells and induction of interleukin-8. Mol. Microbiol. **42:**1337–1348.
11. **Fujikawa, A., et al.** 2003. Mice deficient in protein tyrosine phosphatase receptor type Z are resistant to gastric ulcer induction by VacA of *Helicobacter pylori*. Nat. Genet. **33:**375–381.
12. **Hatakeyama, M.** 2008. Linking epithelial polarity and carcinogenesis by multitasking *Helicobacter pylori* virulence factor CagA. Oncogene **27:**7047–7054.
13. **Higashi, H., et al.** 2002. Biological activity of the *Helicobacter pylori* virulence factor CagA is determined by variation in the tyrosine phosphorylation sites. Proc. Natl. Acad. Sci. U. S. A. **99:**14428–14433.
14. **Iguchi, C., et al.** 2001. Plant polysaccharide PSK: cytostatic effects on growth

and invasion; modulating effect on the expression of HLA and adhesion molecules on human gastric and colonic tumor cell surface. Anticancer Res. **21**:1007–1013.

15. **Jimenez-Soto, L. F., et al.** 2009. *Helicobacter pylori* type IV secretion apparatus exploits beta1 integrin in a novel RGD-independent manner. PLoS Pathog. **5**:e1000684.

16. **Kwok, T., et al.** 2007. *Helicobacter* exploits integrin for type IV secretion and kinase activation. Nature **449**:862–866.

17. **Moese, S., M. Selbach, T. F. Meyer, and S. Backert.** 2002. Cag+ *Helicobacter pylori* induces homotypic aggregation of macrophage-like cells by up-regulation and recruitment of intracellular adhesion molecule 1 to the cell surface. Infect. Immun. **70**:4687–4691.

18. **Montecucco, C., and R. Rappuoli.** 2001. Living dangerously: how *Helicobacter pylori* survives in the human stomach. Nat. Rev. Mol. Cell Biol. **2**:457–466.

19. **Ohnishi, N., et al.** 2008. Transgenic expression of *Helicobacter pylori* CagA induces gastrointestinal and hematopoietic neoplasms in mouse. Proc. Natl. Acad. Sci. U. S. A. **105**:1003–1008.

20. **Oldani, A., et al.** 2009. *Helicobacter pylori* counteracts the apoptotic action of its VacA toxin by injecting the CagA protein into gastric epithelial cells. PLoS Pathog. **5**:e1000603.

21. **Parsonnet, J., et al.** 1991. *Helicobacter pylori* infection and the risk of gastric carcinoma. N. Engl. J. Med. **325**:1127–1131.

22. **Peek, R. M., Jr., and J. E. Crabtree.** 2006. *Helicobacter* infection and gastric neoplasia. J. Pathol. **208**:233–248.

23. **Poppe, M., S. M. Feller, G. Romer, and S. Wessler.** 2007. Phosphorylation of *Helicobacter pylori* CagA by c-Abl leads to cell motility. Oncogene **26**:3462–3472.

24. **Rieder, G., W. Fischer, and R. Haas.** 2005. Interaction of *Helicobacter pylori* with host cells: function of secreted and translocated molecules. Curr. Opin. Microbiol. **8**:67–73.

25. **Schmitt, W., and R. Haas.** 1994. Genetic analysis of the *Helicobacter pylori* vacuolating cytotoxin: structural similarities with the IgA protease type of exported protein. Mol. Microbiol. **12**:307–319.

26. **Schneider, S., C. Weydig, and S. Wessler.** 2008. Targeting focal adhesions: *Helicobacter pylori*-host communication in cell migration. Cell Commun. Signal. **6**:2.

27. **Sharma, S. A., M. K. Tummuru, G. G. Miller, and M. J. Blaser.** 1995. Interleukin-8 response of gastric epithelial cell lines to *Helicobacter pylori* stimulation in vitro. Infect. Immun. **63**:1681–1687.

28. **Tammer, I., S. Brandt, R. Hartig, W. Konig, and S. Backert.** 2007. Activation of Abl by *Helicobacter pylori*: a novel kinase for CagA and crucial mediator of host cell scattering. Gastroenterology **132**:1309–1319.

29. **Tegtmeyer, N., et al.** 2009. Importance of EGF receptor, HER2/Neu and Erk1/2 kinase signalling for host cell elongation and scattering induced by the *Helicobacter pylori* CagA protein: antagonistic effects of the vacuolating cytotoxin VacA. Cell. Microbiol. **11**:488–505.

30. **Viala, J., et al.** 2004. Nod1 responds to peptidoglycan delivered by the *Helicobacter pylori* cag pathogenicity island. Nat. Immunol. **5**:1166–1174.

31. **Wessler, S., et al.** 2000. *Helicobacter pylori* activates the histidine decarboxylase promoter through a mitogen-activated protein kinase pathway independent of pathogenicity island-encoded virulence factors. J. Biol. Chem. **275**:3629–3636.

32. **Yokozaki, H.** 2000. Molecular characteristics of eight gastric cancer cell lines established in Japan. Pathol. Int. **50**:767–777.